References

[1] Gadd, G. E., "Turbulence Damping and Drag Reduction Promoted by Certain Additives in Water," *Nature*, Vol. 206, 1965, p. 463.

[2] Virk, P., "The Toms Phenomenon—Turbulent Pipe Flow of Dilute Polymer Solutions," Sc.D. thesis, 1966, Chemical Engineering Dept., MIT, Cambridge, Mass.

[3] Ellis, A. T., Waugh, J. G., and Ting, R. Y., "Cavitation Suppression and Stress Effects in High-Speed Flows of Water with Dilute Macromolecule Additives," *Transactions of the ASME Journal of Basic Engineering*, Vol. 92, No. 3, Ser. D, Sept. 1970, pp. 459–466.

[4] Fabula, A. G., "An Experimental Study of Grid Turbulence in Dilute High Polymer Solutions," Ph.D. thesis, 1965, Pennsylvania State Univ., University Park, Pa.

[5] Brennen, C. and Gadd, G. E., "Aging and Degradation in Dilute Polymer Solutions," *Nature*, Vol. 215, 1967, p. 1368.

[6] Patterson, R. W., "Turbulence Measurements in Polymer Solutions Using Hot Film Anemometry," Ph.D. thesis, June 1969, Harvard Univ., Cambridge, Mass.

[7] Sherman, B. A., "Effect of Storage on the Drag Reducing Properties of Polyethylene Oxide WSR-301," TN 303/68, 1968, Admiralty Underwater Weapons Establishment, United Kingdom.

[8] McNally, W. A., "Heat and Momentum Transport with Dilute Polyethylene Oxide Solutions," Ph.D. thesis, 1968, Univ. of Rhode Island, Kingston, R. I.

[9] Hoyt, J. W., "A Turbulent Flow Rheometer," *ASME Symposium on Rheology*, ed. by A. W. Morris, June 1965, pp. 71–82.

[10] Librovich, V. B., private communication, Institute of Mechanical Problems, Moscow, USSR.

[11] White, A., "Studies of the Flow Characteristics of Dilute High Polymer Solutions," *Hendon College Research Bulletin*, No. 4, 1967, p. 113.

[12] Lumley, J. L., "Drag Reduction by Additives," *Annual Reviews of Fluid Mechanics*, ed. by W. Sears and M. Van Dyke, Vol. 1, 1969, p. 367.

[13] Barenblatt, G. I., "Turbulence of Anomalous Fluids," *Heat Transfer-Soviet Research*, Vol. 1, 1969, p. 102.

JULY 1972 J. HYDRONAUTICS VOL. 6, NO. 2

Effects of Distributed Injection of Polymer Solutions on Turbulent Diffusion

ROBERT R. WALTERS* AND C. SINCLAIR WELLS JR.†
Advanced Technology Center Inc., Dallas, Texas

Part of an extensive experimental investigation of the mechanics of turbulent diffusion is described for uniformly distributed injection of a polymer solution through a porous wall adjacent to a fully-developed turbulent pipe flow of water. The diffusion data were obtained over an active porous wall section and throughout the region immediately downstream of the porous wall. The previously recorded wall friction anomalies recorded in the region of distributed polymer injection are shown to depend on the viscosity of the resulting polymer solutions near the wall associated with reduced diffusion. Empirical diffusion coefficients give a quantitative determination of the effect of the polymer in reducing turbulent diffusion for the present case. The transitional sublayer was identified from these data as the boundary-layer region requiring polymer to effect wall friction reduction.

Nomenclature

A_i = active porous wall injection area, ft²
ΔB = defined by Eq. (1) using f based on pressure drop only
C = time averaged local concentration of injected tracer in the stream, ppb
C_i = concentration of injected tracer at the wall, ppb
$\bar{C}$ = average bulk concentration of tracer in the stream, $(\dot{w}_i/\dot{w}_t) \times C_i$, ppb
$\bar{C}_p$ = average bulk concentration of the polymer in the main stream, ppm $(\dot{w}_i/\dot{w}_t) \times$ (concentration of polymer injection solution)
D = tube diameter, $2R$, ft
$\mathfrak{D}$ = molecular diffusion coefficient ($\mathfrak{D}_w$ denotes wall condition), ft²/sec
E_D = total diffusivity of mass, $\mathfrak{D} + \epsilon_D$, ft²/sec
f = friction factor, defined as $(R/\rho\bar{u}^2)dP/dx$
g = gravitational constant, ft/sec²
$\dot{m}_0$ = mass flow rate toward tube centerline per unit area at the wall, $(\dot{w}_0/g)$, (lb) (sec)/ft³
P = static stream pressure, psf
R = tube radius, ft
Re_D = Reynolds number, $\bar{u}D/\nu_w$
u = local streamwise velocity, fps
u_1 = stream velocity at tube centerline, fps
u_* = shear velocity, $(\tau_w/\rho)^{1/2}$, fps
$\bar{u}$ = average bulk stream velocity, fps
u^+ = dimensionless velocity variable, u/u_*
$\bar{v}_i$ = average injection velocity through porous wall, fps
w = dimensionless density ratio, ρ_A/ρ, equal to C/C_i
$\dot{w}_i$ = total weight flow rate injected through the porous wall, lbs/sec
$\dot{w}_o$ = total weight flow rate injected through the porous wall, per unit area, 16/ft²·sec
$\dot{w}_t$ = weight flow rate of main stream and injection fluid, lbs/sec
x = streamwise spatial coordinate measured from upstream end of porous wall A, ft

Received September 30, 1970; revision received December 1, 1971. This research was supported by the Office of Naval Research under Contract N 00014-69-C-0214 (Mathematical Sciences Division, Fluid Dynamics Program).

Index category: Hydrodynamics.

* Research Scientist, Fluid Mechanics Group. Member AIAA.

† Manager, Fluid Mechanics Group. Member AIAA.

x' = streamwise distance from downstream end of last active porous wall to tip of sampling probe, ft
y = radial distance from wall of tube, ft
y^+ = dimensionless wall distance variable, yu_*/ν_w
ν_w = kinematic viscosity at the wall, ft²/sec
ρ_A = mass density of injected fluid in the stream, (lbs) (sec²)/ft⁴
ρ = mass density of fluid in the stream, (lbs) (sec²)/ft⁴
τ_w = shear stress at the wall, $(R/2)dP/dx$, psf
ϵ_D = eddy diffusivity of mass, ft²/sec

Introduction

THIS study is part of an extensive experimental investigation of the mechanics of turbulent diffusion for uniformly distributed drag-reducing polymer injection at the wall. Data for this study were obtained with a porous wall injection system used in previous studies.[1] These data have contributed significantly to the physical understanding of the very interesting effects of polymers on turbulent diffusion and associated wall friction anomalies for uniformly distributed polymer injection documented in the initial diffusion experiments.[1]

The object here is to provide a means for predicting the required polymer flux at a wall adjacent to a turbulent flow of water to achieve optimum wall friction reduction. Results from the over all diffusion study have also contributed significantly to the development of techniques for applications of polymer drag reduction to marine vehicles.

The effect of reduced turbulent mass transport in the presence of polymers was shown in Ref. 2 to follow from the reduction of turbulent momentum and heat transport. The effect has been shown experimentally in dilute homogeneous polymer solutions in turbulent pipe flow[3] and has now been well documented experimentally in this laboratory for distributed wall injection.

The experimental study described in Ref. 1 was initiated to obtain empirical data for comparison with the analysis given in Ref. 2 and to investigate the details of turbulent diffusion of polymer additives in the region near the wall. A porous wall apparatus was constructed which adequately provided uniformly distributed polymer injection at very low-injection velocities. Diffusion was found to be greatly reduced in the region near the wall with uniform injection of a polymer solution resulting in much higher injectant concentrations near the wall than found for standard Newtonian diffusion. Also, the transitional sublayer‡ thickness for both momentum and mass transfer showed increases over Newtonian values for distributed injection. This distributed injection system provided drag reduction with a much smaller supply of polymer than required to raise the concentration throughout the shear layer to a drag-reducing level. However, an anomalous pressure drop effect in the vicinity of the active injection system was recorded for these tests and was attributed to a main stream displacement due to the reduced mixing of the injected polymer solution. Later experiments were done to further document the preceding diffusion and pressure drop effects and are reported in the appendices of Ref. 5 for several different variables of the system. The large pressure drop reduction immediately downstream was determined to be a true indication of significant wall friction reduction while the increase in wall friction over the active porous wall was credited to large adverse viscosity effects resulting from reduced polymer diffusion at the wall rather than a significant displacement effect. Wall friction reduction over the distributed injection area was shown to be dependent on polymer mass flux only, a conclusion also made by Hulsebos[6] for porous wall injection of very dilute (50 ppm) polymer solutions. In Wu's experiments[7] with porous wall polymer injection, the system is considered a localized injector while the present case is concerned with distributed injection over an active streamwise section of substantial length. Other polymer diffusion work found in the literature[8,9] was concerned primarily with diffusion far downstream from the point of injection where continued mixing was occurring only in the outer region of the turbulent boundary layer; whereas, the present studies are concerned with the immediate inner wall region affecting the mechanics of wall friction.

The present diffusion data were obtained throughout the region immediately downstream from the porous walls, where the large wall friction reductions were previously recorded, and over the porous wall, a measurement which heretofore had not been made in this apparatus. The analysis of the data provides a quantitative comparison of polymer and water diffusion, as well as defining the boundary-layer region requiring polymer to effect wall friction reduction.

‡ Designation introduced in Ref. 4 for region between viscous sublayer and logarithmic portion of the turbulent boundary layer.

Experimental Setup

The basic porous wall injection apparatus and pipe flow facility used in the experiments discussed herein have been described in detail previously.[1] The basic porous wall injection apparatus utilizes three seamless, sintered stainless steel, smooth cylinders as depicted in Fig. 1. These three porous cylinders, arranged in series, are an integral part of a $\frac{3}{4}$-in. pipe flow facility. The porous wall cylinders used for these experiments were six inches long with a wall thickness of $\frac{1}{4}$ in. and had an approximate porosity of 40% and a pore size of 5μ.

Concentration and velocity profile measurements were made at different downstream distances from the end of the last of the three porous walls; however, porous wall C was the only active section for the present experiments. Streamwise positioning of the probe traversing block was accomplished by using Plexiglas spacers between the traversing block and the end of the last porous wall. For one streamwise set of data the sampling probe tip was extended 0.13 in. into the end of the last porous wall. Pressure drop readings were available across each porous wall as well as immediately downstream and far downstream from the last porous wall.

Concentration and velocity profile data were obtained with a total head probe 0.014 in. o.d. and 0.010 in. i.d., having a bleed hole whereby a sample of the stream fluid was slowly collected in a decontaminated glass test tube at each radial position from the wall of the pipe after obtaining a total pressure reading. The percentage of the injection fluid in the main stream samples was based on the fluorometric method of using a fluoroscien tracer (Uranine B) mixed with the injection fluid in the injection fluid reservoir at a concentration of 10 ppm. The tracer concentration in the stream

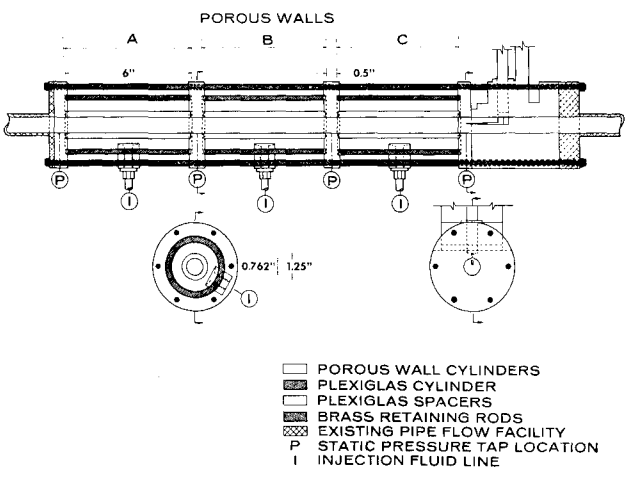

Fig. 1 Schematic of the wall injection system.

samples, referenced to a sample of the injection fluid, was measured by a Beckman Ratio Fluorometer, Model 772, accurate in detecting tracer solution concentrations of two parts per billion.

The pressure taps and total head probe were connected to a variable-reluctance transducer, the signal from which was displayed on a digital voltmeter via a carrier amplifier. Flow rates of the main water stream, obtained from the local municipal water supply, were determined by using a weigh tank at the exit water jet. The main stream water temperature and injectant temperature were recorded for each run, as well as the viscosity for each polymer solution. Viscosities were measured with a Contraves viscometer using an MS-O concentric cylinder measuring system at shear velocities comparable to the experimental values used. The viscosity reading for each solution was then extrapolated to the shear velocities of the experiments.

No corrections were determined for possible adverse effects of the polymer on the total head probe and static port readings. The integrated flow rates from the velocity profiles were in excellent agreement with the measured flow rates with an average difference of 1% for the polymer data and 0.15% for the water data. However, if an adverse effect is occurring in the immediate wall region or elsewhere, this would not alter the primary measurements, the concentration profile readings.

Experimental Results

Initial Selection of Test Variables

From the results of prior tests,[5] two polymer mass injection rates were selected that would demonstrate two effects previously observed: 1) increased wall friction over the first injection section; and 2) a "wall effect," where the wall friction reduction immediately downstream from the active porous wall would be greater than for the resultant homogeneous polymer concentration far downstream. The desired polymer mass flux was supplied by two different concentration solutions to study the effects of injected polymer solution concentration and viscosity variation.

The two polymer (POLYOX WSR-301) concentrations were the same as those used in previous tests, 1000 ppm and 5000 ppm, a factor of 5 variations in concentration and approximately a factor of 3 variation in solution viscosity at the present shear velocity.

The two polymer mass injection rates resulted in a bulk polymer stream concentration of 2 ppm and 0.4 ppm, and are referred to in the following discussions as high and low polymer mass flux, respectively. The high and low polymer mass flux corresponds to an injection to stream velocity ratio, $\bar{v}_i/\bar{u}$, of 1.5×10^{-4} and 3×10^{-5} for the 1000 ppm solution and 3×10^{-5} and 6×10^{-6} for the 5000 ppm solutions.

During the initial experiments, variations in diffusion were found as a result of polymer solution age. The only physical difference observed between the solutions increasing in age was a decrease in the pituitousness or "stringiness" of the solution which is a qualitative indication of the solution's viscoelastic nature. Consequently, 2 days and 5 days were selected for solution age variation, the former being approximately the minimum time for the polymer to fully disperse in the solvent (water), while the latter age allowed time for a significant change in the pituitousness of the solution. Data were taken for age variations of the 5000 ppm polymer solution only. The effects of polymer solution age are presented succinctly herein by a comparison of the total diffusivity of mass coefficients calculated from velocity and concentration profile data.

The main stream velocity was maintained at 13 fps while pressure drop and velocity and concentration profile measurements were made for two injection rates of water and for the three polymer solutions. The polymer solutions were all identically mixed using a slow agitation in local municipal tap water containing approximately 0.1 ppm of chlorine. Solutions were exposed to atmospheric conditions and mixed occasionally to agitate suspended polymer that settled to the bottom of the mixing containers.

Pressure Drop Measurements

The pressure drop or wall friction data are plotted in terms of ΔB in Fig. 2, where wall friction reduction is indicated by positive values of ΔB. The ΔB relationship used here, which Meyer[10] used to correlate pressure drop data for polymer solutions with the shear velocity, u^*, is as follows:

$$\Delta B = (2)^{1/2}[1(f)^{1/2} - 4\log_{10}Re_D(f)^{1/2} + 0.39] \quad (1)$$

where the Reynolds number is calculated using the wall viscosity. The right side of this equation is zero for Newtonian, smooth-wall pipe flow data.

The open symbols in Fig. 2 are data computed assuming water viscosity at the wall and the closed symbols over the active porous wall are data computed assuming polymer injection solution viscosity at the wall. Since the true viscosity in the wall region over the porous wall was not known, the water viscosity and polymer injection solution viscosity

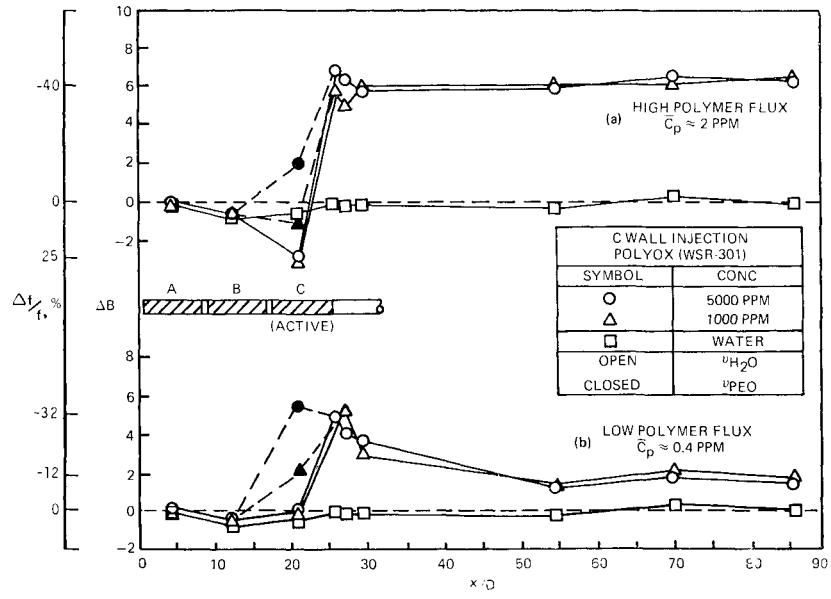

Fig. 2 Streamwise drag-reduction data associated with the downstream concentration profiles for two different concentrations of polymer injection fluid.

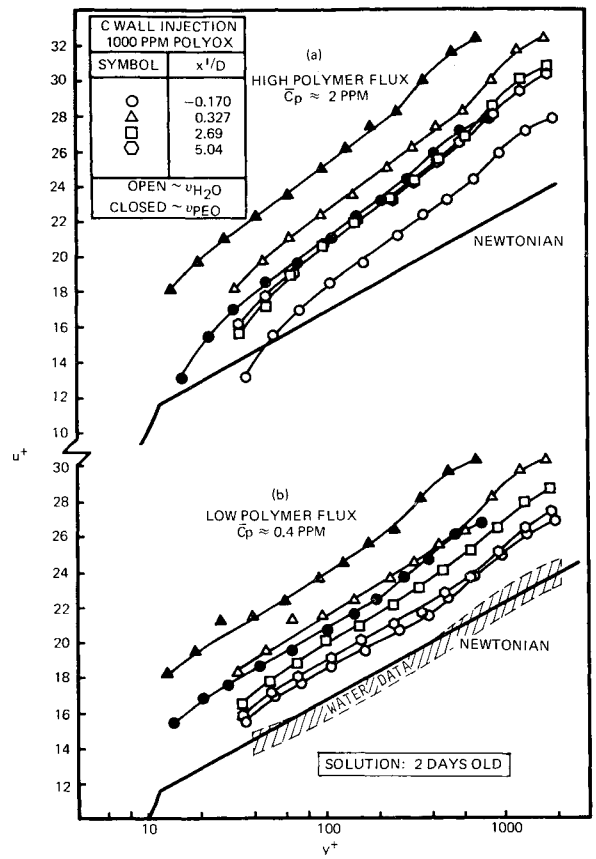

Fig. 3 Nondimensionalized downstream velocity profiles for the high and low injection rates of fresh 1000 ppm POLYOX through the *C* wall.

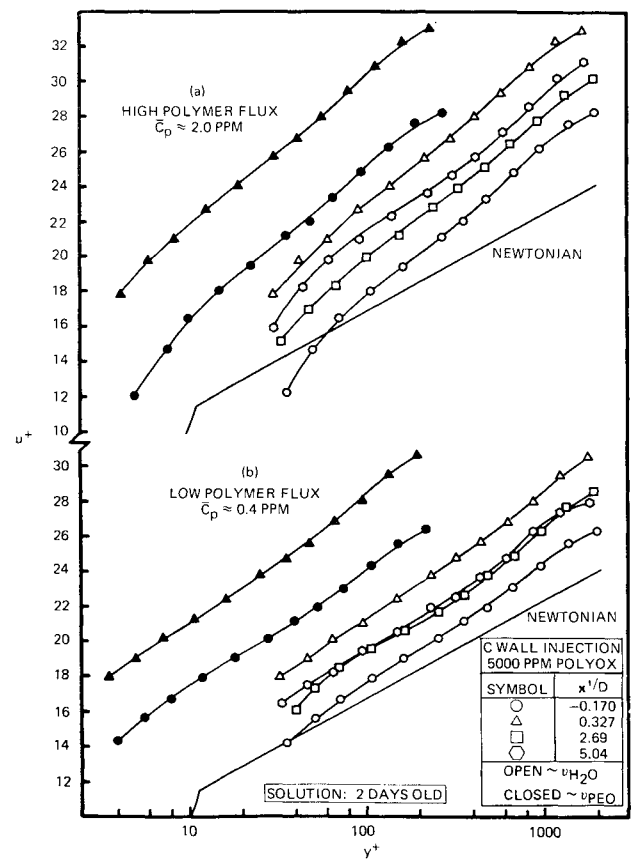

Fig. 4 Nondimensionalized velocity profiles for the high and low injection rates of 5000 ppm POLYOX through the *C* wall.

were used as the respective minimum and maximum possible wall viscosities.

The wall friction deviations for both concentrations are almost identical. The two effects of increased wall friction over the active section and the downstream "wall effect" are shown in Fig. 2 for high and low polymer flux, respectively. The ΔB values at 86 diam downstream from the reference position average 6.5 and 1.6 for high and low polymer mass injection, respectively. The corresponding range of ΔB values obtained from the $\frac{1}{4}$ in. homogeneous solution pipe flow data at the same shear velocities and same equivalent high and low polymer concentrations are 5.0–5.6 and 1.2–1.7. This is an indication of negligible effective degradation of polymer solutions passing through the porous wall and the shear layer for these conditions. The water data shown in Fig. 2 indicate less than 5% deviation of the friction factor from theoretical values for Newtonian, smooth-wall pipe flow. The percent friction factor deviation corresponding to the respective ΔB values are indicated in Fig. 2.

Velocity Profiles

The velocity profile data are presented here in terms of the "law of the wall" parameters, u^+ and y^+, related by the inner wall velocity profile equation,[11]

$$u^+ = 5.75 \log_{10} y^+ + 5.5 \qquad (2)$$

where the constants have been determined from Newtonian, smooth-wall pipe flow data.

The sublayer velocity profile is presented simply by equating u^+ and y^+. A velocity profile for the transitional sublayer region is not shown; however, the intersection of the sublayer and turbulent region curves is shown here for a reference to the Newtonian transition region.

The present velocity data for water injection, as indicated in Fig. 3, are in good agreement with the preceding logarithmic expression. The velocity profiles for high and low polymer mass injection of two-day old, 1000 ppm and 5000 ppm solutions are depicted in Figs. 3 and 4, respectively. The downstream u_* values were computed from local pressure drop data while the local u_* value for the profile over the end of the active section was determined from a data plot of a pressure drop vs active porous wall length.

A significant deviation from the straight line turbulent core data is considered to be indicative of approaching the transitional sublayer region as described in previous work.[1] This deviation is evident in the high polymer mass flux data obtained over the active wall. The height of the transitional sublayer thickness is indicated by the y^+ value, which is viscosity dependent; however, comparison data are shown using polymer solution viscosity for the profiles over the porous wall and immediately downstream. The viscosity effects will be discussed in more detail in a later section.

The nondimensional profiles for high polymer flux also indicate a change in the slope of the turbulent core region of the curve, traditionally denoting a decrease in the turbulent mixing length or mixing coefficient. Changes in velocity profile slope for the lower polymer flux are more subtle and not as evident as in the higher polymer flux data.

Concentration Profiles

The local stream concentration was nondimensionalized with the average bulk stream concentration, $C/\bar{C}$ (the ratio of the tracer concentrations is assumed to be identical to the polymer concentration ratio for polymer solution injection). For water injection, the concentration profile data correlated for three different injection rates at each streamwise position when nondimensionalized with $\bar{C}$. The correlated water data are shown in Figs. 5 and 6. These water data show the concentration profiles approaching the fully-mixed ratio of 1 for each successive downstream position. Good agree-

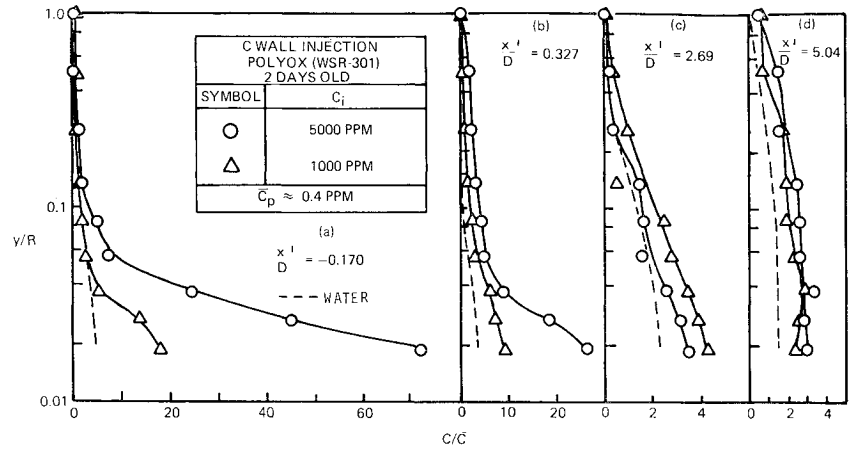

Fig. 5 Downstream diffusion effects for equal high polymer injection.

ment was found between the $\bar{C}$ calculated from the known flowmeter output, the $\bar{C}$ determined from an integration of the concentration profiles and the $\bar{C}$ measured by the fluorometric technique from a sample collected at the test pipe exit in the weigh tank, for all downstream positions. The $\bar{C}$ comparison data are tabulated in Ref. 5 for both water and polymer injection data.

The concentration profiles for the two-day old, 5000 ppm polymer solution are compared to those of the two-day old 1000 ppm polymer solution at the high and low polymer mass flux in Figs. 5 and 6 for the four different downstream positions. A significant difference in the concentration profiles is found between data taken over the porous wall and the position $\frac{1}{4}$ in. downstream where all previous concentration profile data had been obtained, indicating the continuous active wall injection serves to retain the polymer near the wall. For a streamwise distance of $\frac{1}{2}$ pipe diameter, the measured concentration near the wall changed by a factor of 5, traversing from the active to an inactive section. Over the wall, the polymer concentration is maintained at a higher level in the near-wall region for the high concentration injectant at both the high and low equal polymer mass flux conditions. The downstream diffusion appears to be more dependent on polymer mass flux than the injectant concentration or age, since a significant concentration gradient was found up to five diameters downstream for high polymer flux and not for the low polymer flux case.

Data Analysis

The data were examined and correlated in terms of previous analyses to determine: 1) the effects of the wall viscosity on transitional sublayer height and wall friction, 2) the region in the shear layer where the polymer is effective in reducing wall friction; and 3) the quantitative reduction in the turbulent diffusion coefficient across the shear layer.

Viscosity Effects

Using the concentrated injectant solutions of 1000 and 5000 ppm polymer, with respective viscosities 2.1 and 7.6 times greater than water ($\nu_w = 0.9 \times 10^{-5}$ ft^2/sec) at the present shear velocity, the effects attributed to viscosity in previous experiments[1] were presently more pronounced and were studied in greater detail. The present polymer concentration profile data over the active wall depict high polymer concentrations near the wall, as discussed in the previous sections, sufficient to be attended by an increased viscosity in this region. A power-law curve fit of the profiles for $y/R < 0.1$ provided a crude indication of the injection concentrations existing some finite distance above the wall in the viscous sublayer.

The polymer injectant viscosity was therefore used to recompute the present friction data. A limited friction reduction and, in some cases, an increase in wall friction over the active wall are indicated in the ΔB data based on water viscosity, shown in Fig. 2; however, this friction increase can be well accounted for using the viscosity of the polymer injectant as shown by the closed symbols.

The polymer injectant and the water viscosities, as mentioned previously, provided the two extremes of the viscosity range for a data analysis. The polymer solution viscosity and attendant solution viscosity in the immediate wall region, based on the concentration profiles, were different for the different polymer injection cases, even for the same injectant concentration.

Due to the uncertainty of determining an "effective" wall viscosity, the maximum and minimum viscosities (polymer

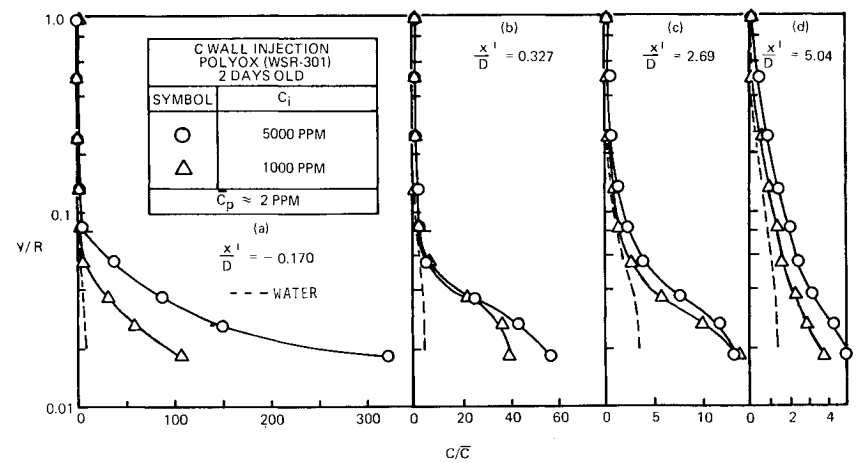

Fig. 6 Downstream diffusion effects for equal low polymer injection.

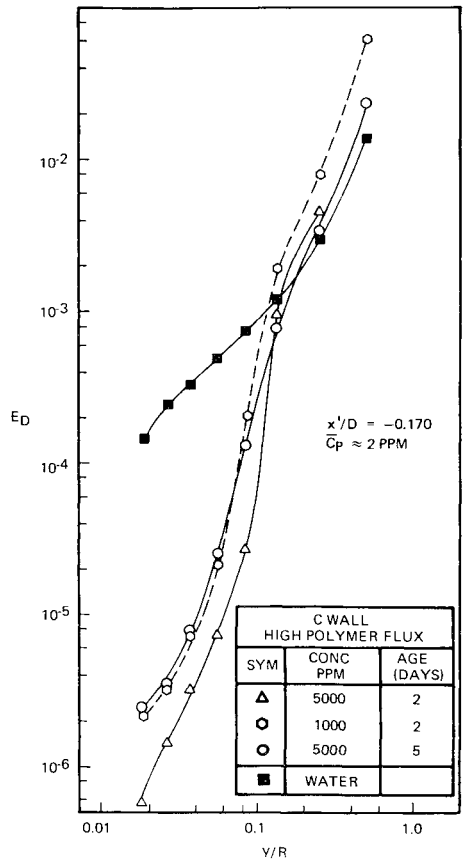

Fig. 7 Total diffusivity of mass calculated for data over active porous wall for a high polymer flux.

injectant solution and water, respectively) were used to show maximum possible effects of viscosity on the wall friction and momentum and diffusion transitional sublayer thickness. Taking into account the maximum possible viscosity effect, there is not clear evidence of an increased momentum transitional sublayer since the velocity profiles based on polymer injectant viscosity have shifted to the left a significant amount in Figs. 3 and 4 where the y^+ values for the profile deviation from a straight line are equal to or less than y^+ values one would normally expect for the water data also. There is, however, a clear indication of an increased diffusion transitional sublayer thickness after accounting for the maximum viscosity effects. The edge of the transitional diffusion sublayer was estimated to extend over the y^+ range of 30–100 depending on the value of wall viscosity used; whereas, for water the y^+ value was approximately 5, based on the analysis by Deissler.[12] The edge of the transitional diffusion sublayer is indicated by a significant change in slope from the straight line of the turbulent core region on a nondimensionalized concentration profile plot.

Effective y^+

The region of the shear layer in which the polymer first becomes effective in reducing wall friction was identified from these data by matching the local friction reduction, accounting for the entrance length and a viscosity effect, over the porous wall to a polymer concentration in the concentration profile. This match was based on friction reduction vs polymer concentration data for homogeneous polymer solutions at the same shear velocities. The local porous wall friction reduction was determined from a data plot of pressure drop vs active porous wall length. The data in Ref. 5 indicate that the entrance length effects diminish over a streamwise length of one active porous wall, therefore placing the present profile over the wall at the downstream edge of this entrance length. The height above the wall was related in terms of the y^+ parameter to account for wall viscosity. Using this matching technique, the data show that the effective region occurs in the transitional sublayer, or over the y^+ range of 10-80, outside the viscous sublayer.

Diffusion Equation

To obtain a quantitative determination of the effect of the polymer in reducing turbulent diffusion, the diffusion equation from Ref. 13 was rewritten in terms of a diffusion coefficient, E_D. The coefficient E_D is the combination of the molecular diffusion coefficient and the turbulent diffusion coefficient or eddy diffusivity of mass. This was necessary since the two coefficients could not be determined separately unless a value was assumed for the molecular diffusion coefficient of the concentrated polymer solutions. An estimated molecular diffusion coefficient is listed by Poreh and Hsu[14] for POLYOX WSR-301, based on the Mandelkern and Flory model, for use in the viscous sublayer; however, the present data were obtained only to the edge of the transitional sublayer region. Also, the diffusion reductions in the previous sections have been referred to as turbulent diffusion reductions since the magnitude of the diffusion coefficients determined by the following analysis is several orders of magnitude above standard Newtonian molecular diffusion. In addition, the slope of the velocity profile for the turbulent core indicates reduced turbulent mixing. Therefore, the reductions to be shown in E_D are attributed for the most part to reductions in the eddy diffusivity of mass.

The diffusion coefficient was found by the derivation of the following differential diffusion equation for the local, time-average stream concentration, given by:

$$\partial\rho_A/\partial t + \nabla\cdot\rho_A\bar{U} = (\nabla\cdot\rho\mathfrak{D}\nabla w) \tag{3}$$

where $w = \rho_A/\rho$ and $\bar{U}$ is the local, time-averaged velocity vector. For axisymmetric diffusion from distributed injection at the wall of a pipe containing a steady-state, fully-developed turbulent flow, assuming the streamwise diffusion to be small in comparison with the transverse diffusion, Equation (3) can be simplified and written in terms of the wall coordinates as:

$$(R - y)u(\partial w/\partial x) = (\partial/\partial y)[(R - y)E_D(\partial w/\partial y)] \tag{4}$$

where the molecular diffusivity $\mathfrak{D}$ is replaced by the total diffusivity of mass coefficient, E_D, for turbulent flow. This equation can be written in terms of E_D to obtain a direct determination of the mass transfer coefficient from the measured concentration profiles.

After integrating Eq. (4) with respect to y it becomes:

$$E_D(y) = \left[\int_0^y (R - y)u\left(\frac{\partial w}{\partial x}\right) dy + R\mathfrak{D}_w\left(\frac{\partial w}{\partial y}\right)_w\right] \Big/ (R - y)\left(\frac{\partial w}{\partial y}\right)_y \tag{5}$$

where the second term on the right is negligible for the present inactive wall case but is equal to the solution mass flux at the wall, $\dot{m}_o/\rho = -\mathfrak{D}_w(dw/dy)_w$, for an active injection section.

Empirical Diffusion Coefficients

The concentration profile data, measured over the end of the last porous wall, was used to evaluate E_D for active injection. Since the location was at the end of the porous wall where an equilibrium condition had been indicated, the $\partial w/\partial x$ was assumed negligible compared to the wall mass flux term for a localized computation. The E_D values depicted in Fig. 7 were therefore computed from the concentra-

tion profile data, allowing the first term on the right side of Eq. (5) to be zero.

The decreased diffusion for polymer injection, implied by the changes in the concentration profiles, is denoted numerically by the calculated differences in the mass transfer coefficient, E_D, between polymer and water injection. The mass transfer coefficient has not been nondimensionalized with respect to the kinematic wall viscosity due to the uncertainty of determining an exact effective wall viscosity. The mass transfer coefficient therefore has dimensions of ft^2/sec.

The diffusion rate in the wall region, as presented by E_D, decreased by two orders of magnitude for the high polymer mass flux case compared to water injection, down to a diffusion level less than two orders of magnitude above the molecular diffusion level of water for the closest wall measurements plotted in Fig. 7. The two different 5000 ppm polymer solutions react almost identically in the severe mixing of the outer turbulent core region over the wall (see Fig. 7) as they also do downstream of injection, as in Fig. 8; whereas, in the critical region approaching the transitional sublayer over the active wall, the differences in the viscoelastic properties of the injectants become apparent in the diffusion rates. It should be pointed out here that the five-day old, 5000 ppm polymer solution and the two-day old, 1000 ppm polymer solution were injected at the same polymer mass flux corresponding to a solution mass flux ratio of five; however, the diffusion rate near the wall is shown to be the same for both. It is hypothesized that the viscosity effects are about the same for these two injection conditions basing the effective wall viscosity on the polymer mass flux. The difference between these two solutions and the two-day old 5000 ppm polymer solution could be due to stresses other than the viscous stresses since the latter is more viscoelastic in appearance than the former two injectant solutions.

At a low polymer mass flux the differences between the three injectant polymer solutions were distinct near the wall and gradually diminished in the fully-turbulent core. The polymer diffusion, for all three low polymer flux cases over the wall, was an order of magnitude less than water diffusion. The change in polymer characteristics due to age also resulted in a significant change in the diffusion near the wall at the lower polymer flux.

For the polymer diffusion cases, the diffusion rate in the region of the polymer deficient turbulent core is greater than the Newtonian or water diffusion case. This follows from the very small concentration gradients in this region which lacks a supply of polymer from the vicinity of the polymer-laden sublayer due to an apparent breakdown in the normal turbulent transport mechanism in the general region of the transitional sublayer.

At the farthest downstream position, as shown in Fig. 8, the polymer diffusion near the wall is still reduced by an order of magnitude. From previous data, little distinction can be made between the water and polymer injection after 9 pipe diameters downstream. It was in the vicinity of $x'/D < 5$ that the maximum wall friction reduction occurred for most cases previously discussed while after 9 pipe diameters the wall friction was similar to the fully-mixed homogeneous solution downstream. This indicates that the effect is due to a greater polymer concentration in the effective y^+ region than in the bulk of the far downstream region.

Only data for the high polymer mass flux were presented here due to the similar nature of the plots for the two injection cases. The low injection case differed only in a slightly reduced turbulent diffusion reduction effectiveness.

This study has answered some of the original questions about wall friction anomalies over the active porous wall by making the effects more pronounced and studying them in more positive detail. Continued studies are now needed to optimize the wall friction reduction by minimizing the wall viscosity effect using variations in the injectant solution viscosity. The data obtained over the porous wall proved to

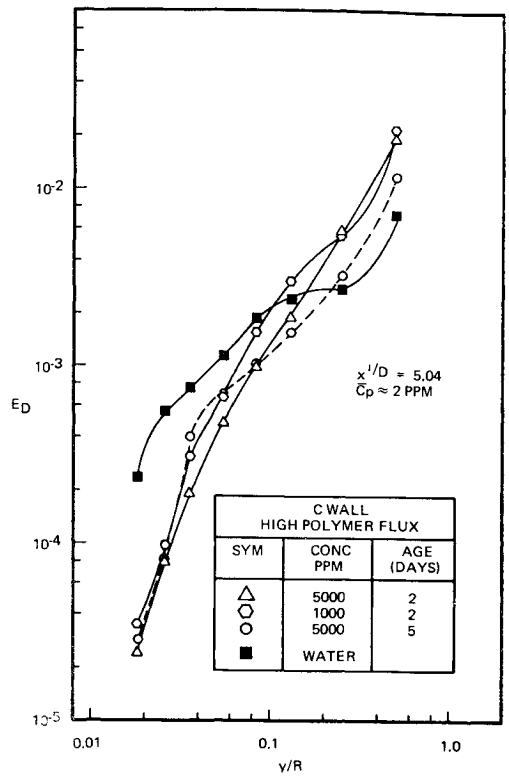

Fig. 8 Total diffusivity of mass calculated from data downstream of an active porous wall for high polymer flux.

be useful in predicting full-scale external boundary layer anomalies; however, experiments to obtain more than one streamwise position over the active wall are needed for determining simultaneous momentum and mass transfer characteristics.

Conclusions

The following conclusions are presented based on the experimental study of the mechanics of turbulent diffusion described herein for the uniform injection of polymer solutions made from a single grade of polymer.

1) Wall friction reduction over the porous wall is dependent on polymer mass flux rather than solution mass flux, the former having a maximum effective value over the porous wall. A wall friction increase over an active porous wall for certain conditions of high polymer mass flux was attributed to the attendant high wall viscosities. When changes in wall friction were examined in terms of ΔB, based on the viscosity of the polymer injection solution, friction reduction was indicated.

2) A significant increase in measured wall friction reduction occurs over inactive sections immediately downstream from an active porous wall injecting concentrated polymer solutions. This is due in part to an apparent increase, compared to the active section, in transport of polymer to a critical shear layer region where the polymer becomes effective in reducing wall friction. Also, due to the diminished supply of concentrated polymer at the wall at this immediate downstream position, the deleteriously high wall viscosity is consequently reduced; whereas, the concentrated polymer in the critical wall region is still not fully-diluted to the downstream bulk concentration.

3) The critical shear region, where the polymer becomes effective in reducing wall friction, was estimated to extend into the transitional sublayer region for the y^+ range of 10–80 over the active porous wall, the approximate region where the magnitude of the turbulence production and dissipation

has been found by others to approach a maximum for standard Newtonian fully-developed turbulent flow.

4) The significant reduction in turbulent diffusion for uniform injection of polymer solutions at the wall is reflected in a one to two order of magnitude reduction in the total diffusivity of mass resulting in much higher concentrations as compared to water injection for the same radial distances above the wall ($y^+ \leq 150$, $y/R \leq 0.1$). The turbulent diffusion near the wall decreases for an increase in the polymer solution concentration or an increase in the polymer mass flux through the wall, the latter being slightly more effective.

5) The total diffusivity of mass was reduced by an order of magnitude in the downstream region from the active porous wall where a significant reduction in wall friction was measured.

6) Calculation of both the nondimensionalized heights of the apparent momentum and diffusion transitional sublayer regions and the true reduction of turbulent shear stresses is complicated by the difficulty in determining an "effective" wall viscosity over an active polymer injection section.

References

[1] Walters, R. R. and Wells, C. S., "An Experimental Study of Turbulent Diffusion of Drag-Reducing Additives," *Journal of Hydronautics*, Vol. 5, No. 2, April 1971, pp. 65–77.

[2] Wells, C. S., "An Analysis of Uniform Injection of a Drag-Reducing Fluid into a Turbulent Boundary Layer," *Viscous Drag Reduction*, Proceedings of the Symposium in Dallas, Texas, Sept. 1968, Plenum Press, New York, 1969, pp. 361–382.

[3] Suraiya, T., *Mass Transfer to Dilute Polymer Solutions in Turbulent Pipe Flow*, B.S. thesis, 1968, MIT, Cambridge, Mass.

[4] Granville, P. S., "The Frictional Resistance and Velocity Similarity Laws of Drag-Reducing Dilute Polymer Solutions," *Journal of Ship Research*, Vol. 12, 1968, p. 201.

[5] Walters, R. R. and Wells, C. S., "Effects of Distributed Injection of Polymer Solutions on Turbulent Diffusion," Rept. B-94000/1CR-7, March 1971, Advanced Technology Center Inc., Dallas, Texas.

[6] Hulsebos, J., *An Investigation of a Turbulent Boundary Layer with Homogeneous Polymer Injection*, Ph.D. thesis, 1968, Georgia Institute of Technology, Atlanta, Ga.

[7] Wu, J., "Some Techniques of Injecting Additive Solutions for Drag Reduction," TR 7101-1, Feb. 1971, Hydronautics Inc., Laurel, Md.

[8] Wetzel, J. M. and Ripken, J. F., "Shear and Diffusion in a Large Boundary Layer Injected with Polymer Solution," Rept. 114, Feb. 1970, St. Anthony Falls Hydraulic Lab., University of Minnesota, Minneapolis, Minn.

[9] Fabula, A. G. and Burns, T. J., "Dilution in a Turbulent Boundary Layer with Polymeric Drag Reduction," TP 171, 1970, Naval Undersea Research and Development Center, Pasadena, Calif.

[10] Meyer, W. A., "A Correlation of the Frictional Characteristics for Turbulent Flow of Dilute Viscoelastic Non-Newtonian Fluids in Pipes," *AIChE Journal*, Vol. 12, No. 3, 1966, pp. 522–525.

[11] Schlichting, H., *Boundary Layer Theory*, 5th ed., McGraw-Hill, New York, 1970, p. 508.

[12] Deissler, R. G., "Analysis of Turbulent Heat Transfer, Mass Transfer and Friction in Smooth Tubes at High Prandtl and Schmidt Numbers," Rept. 1210, 1955, NACA.

[13] Bird, R. B., Stewart, W. E., and Lightfoot, E. N., *Transport Phenomena*, 2nd Printing, Wiley, New York, 1962, p. 557.

[14] Poreh, M. and Hsu, K. S., "Diffusion of Drag-Reducing Polymers in a Turbulent Boundary Layer," Rept. 125, April 1971, Iowa Institute of Hydraulic Research, Univ. of Iowa, Iowa City, Iowa.